Densovirus associated with sea-star wasting disease and mass mortality

Ian Hewson[a,1], Jason B. Button[a], Brent M. Gudenkauf[a], Benjamin Miner[b], Alisa L. Newton[c], Joseph K. Gaydos[d], Janna Wynne[e], Cathy L. Groves[f], Gordon Hendler[f], Michael Murray[g], Steven Fradkin[h], Mya Breitbart[i], Elizabeth Fahsbender[i], Kevin D. Lafferty[j], A. Marm Kilpatrick[k], C. Melissa Miner[k], Peter Raimondi[k], Lesanna Lahner[l], Carolyn S. Friedman[m], Stephen Daniels[n], Martin Haulena[o], Jeffrey Marliave[o], Colleen A. Burge[m,p,2], Morgan E. Eisenlord[p], and C. Drew Harvell[p]

[a]Department of Microbiology, Cornell University, Ithaca, NY 14853; [b]Department of Biology, Western Washington University, Bellingham, WA 98225; [c]Zoological Health Program, Wildlife Conservation Society, Bronx, NY 10460; [d]School of Veterinary Medicine, University of California, Davis, CA 95616; [e]California Science Center, Los Angeles, CA 90089; [f]Natural History Museum of Los Angeles County, Los Angeles, CA 90007; [g]Monterey Bay Aquarium, Monterey, CA 93940; [h]Olympic National Park, National Parks Service, Port Angeles, WA 98362; [i]College of Marine Science, University of South Florida, St. Petersburg, FL 33701; [j]Western Ecological Research Center, US Geological Survey c/o Marine Science Institute, University of California, Santa Barbara, CA 93106; [k]Department of Ecology & Evolutionary Biology, University of California, Santa Cruz, CA 95064; [l]Seattle Aquarium, Seattle, WA 98101; [m]School of Aquatic & Fishery Sciences, University of Washington, Seattle, WA 98195; [n]Department of Physiology and Neurobiology, University of Connecticut, Storrs, CT 06269; [o]Vancouver Aquarium, Vancouver, BC, Canada V6G 3E2; and [p]Department of Ecology & Evolutionary Biology, Cornell University, Ithaca, NY 14853

Edited by James L. Van Etten, University of Nebraska-Lincoln, Lincoln, NE, and approved October 21, 2014 (received for review August 28, 2014)

Populations of at least 20 asteroid species on the Northeast Pacific Coast have recently experienced an extensive outbreak of sea-star (asteroid) wasting disease (SSWD). The disease leads to behavioral changes, lesions, loss of turgor, limb autotomy, and death characterized by rapid degradation ("melting"). Here, we present evidence from experimental challenge studies and field observations that link the mass mortalities to a densovirus (*Parvoviridae*). Virus-sized material (i.e., <0.2 μm) from symptomatic tissues that was inoculated into asymptomatic asteroids consistently resulted in SSWD signs whereas animals receiving heat-killed (i.e., control) virus-sized inoculum remained asymptomatic. Viral metagenomic investigations revealed the sea star-associated densovirus (SSaDV) as the most likely candidate virus associated with tissues from symptomatic asteroids. Quantification of SSaDV during transmission trials indicated that progression of SSWD paralleled increased SSaDV load. In field surveys, SSaDV loads were more abundant in symptomatic than in asymptomatic asteroids. SSaDV could be detected in plankton, sediments and in nonasteroid echinoderms, providing a possible mechanism for viral spread. SSaDV was detected in museum specimens of asteroids from 1942, suggesting that it has been present on the North American Pacific Coast for at least 72 y. SSaDV is therefore the most promising candidate disease agent responsible for asteroid mass mortality.

virus | Asteroidea | disease | densovirus | wasting

Since June 2013, millions of sea stars (asteroids) of the west coast of North America have wasted away into slime and ossicle piles, due to a disease known as sea-star wasting disease (SSWD). SSWD has been used to collectively describe die-offs of sea stars in the Northeast Pacific since at least 1979; however, this SSWD event differs from other asteroid mass mortalities (1–5) due to its broad geographic extent (from Baja California, Mexico to Southern Alaska; pacificrockyintertidal.org) and many ($n = 20$) species affected, representing several major lineages of Asteroidea (Fig. 1, Table S1, and *SI Text*). The extensive geographic range and number of species infected might make SSWD the largest known marine wildlife epizootic to date. Outward signs of SSWD vary slightly among species but generally start with behavioral changes, including lethargy and limb curling, followed by lesions, ray autotomy, turgor loss (deflation), and end with animal death (Fig. 1). Histology of dead and dying asteroids from geographically widespread natural habitats and aquaria, showed epidermal necrosis and ulceration, and dermal inflammation and edema in the body wall. Clinically affected (i.e., symptomatic) individuals rarely recover in the laboratory and only occasionally in the field.

The cause of SSWD remains a mystery. Scientific hypotheses given for other asteroid mortality events include storms (6–11), temperature anomalies (1, 3, 12), starvation (13), and infection by unidentified pathogens (5). For instance, pathogens in the bacterial genus *Vibrio* (12, 14, 15) and an unidentified eukaryotic parasite (4) were seen in die-offs of the tropical asteroid *Acanthaster planci* and the Mediterranean asteroid *Astropecten jonstoni*. However, it is difficult to distinguish the cause of an infectious disease from the associated microbial community that can flourish in a sick or injured animal.

Some early patterns from the field supported the hypothesis that SSWD is contagious. Within a region, SSWD has sometimes moved from site to site similar to an infectious disease. For example, the disease spread north to south in Southern California. All of the major aquaria on the North American Pacific Coast

Significance

Sea stars inhabiting the Northeast Pacific Coast have recently experienced an extensive outbreak of wasting disease, leading to their degradation and disappearance from many coastal areas. In this paper, we present evidence that the cause of the disease is transmissible from disease-affected animals to apparently healthy individuals, that the disease-causing agent is a virus-sized microorganism, and that the best candidate viral taxon, the sea star-associated densovirus (SSaDV), is in greater abundance in diseased than in healthy sea stars.

Author contributions: I.H. and B.M. designed research; I.H., J.B.B., B.M.G., B.M., A.L.N., J.K.G., J.W., C.L.G., G.H., M.M., S.F., E.F., C.M.M., P.R., L.L., S.D., M.H., J.M., C.A.B., M.E.E., and C.D.H. performed research; I.H., J.B.B., B.M.G., M.B., K.D.L., A.M.K., and C.S.F. analyzed data; I.H., J.B.B., B.M.G., B.M., A.L.N., G.H., M.M., M.B., K.D.L., A.M.K., C.M.M., P.R., C.S.F., M.H., C.A.B., M.E.E., and C.D.H. wrote the paper; I.H. is senior author; I.H., J.B.B., B.M.G., and E.F. analyzed genomic data; I.H., C.A.B., and M.E.E. performed viral challenge experiments; I.H. and J.B.B. performed molecular biological analyses; B.M., J.W., M.M., S.F., C.M.M., P.R., L.L., M.H., J.M., C.A.B., and C.D.H. collected samples; B.M., J.K.G., J.W., M.M., S.F., C.M.M., P.R., L.L., M.H., J.M., C.A.B., and C.D.H. made field observations; A.L.N. and S.D. performed histological and microscopic examination; I.H., J.K.G., M.B., and C.S.F. interpreted results; I.H., C.L.G., and G.H. analyzed museum specimens; and I.H., K.D.L., and A.M.K. performed statistical analyses.

The authors declare no conflict of interest.

This article is a PNAS Direct Submission.

Freely available online through the PNAS open access option.

Data deposition: The sequence reported in this paper has been deposited in the GenBank database (accession no. PRJNA253121).

[1]To whom correspondence should be addressed. Email: hewson@cornell.edu.

[2]Present address: Institute for Marine and Environmental Technology, University of Maryland, Baltimore County, Baltimore, MD 21202.

This article contains supporting information online at www.pnas.org/lookup/suppl/doi:10.1073/pnas.1416625111/-/DCSupplemental.

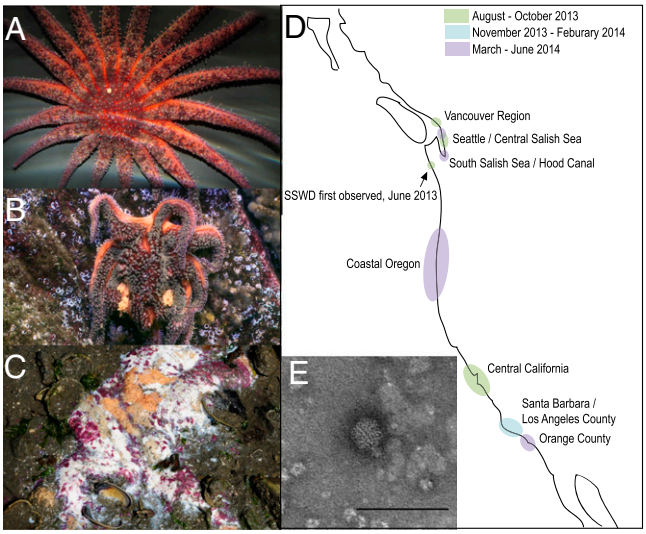

Fig. 1. Photographs of SSWD-affected stars (*A*) asymptomatic *P. helianthoides*, (*B*) symptomatic *P. helianthoides*, and (*C*) symptomatic *P. ochraceus*. Disease symptoms are consistent with loss of turgor, loss of rays, formation of lesions, and animal decomposition. (*D*) Map showing occurrence of SSWD based on first reported observation. (*E*) Transmission electron micrograph of negatively stained (uranyl acetate) viruses extracted from an affected wild *E. troschelii* from Vancouver . The sample contained 20–25-nm diameter nonenveloped icosohedral viral particles on a background of cellular debris (primarily ribosomal subunits) and degraded viral particles of similar morphology. (Scale bar: 100 nm.)

were affected by SSWD in Fall 2013, with mass mortality of captive asteroids. However, SSWD did not spread into aquaria that sterilize inflowing seawater with UV light but did spread into nontreated aquaria. Furthermore, the incursion of SSWD in aquaria with sand-filtered intake suggests a microscopic infectious stage, rather than a disease that spread only via contact with an infected host or vector. Overall, these patterns suggest a microscopic, water-borne, infectious disease agent, rather than environmental pollutants.

Inoculation with Virus-Sized Homogenates Induces Wasting-Disease Signs

We turned to viruses as potential infectious agents in SSWD because histologic evaluation of hundreds of slides indicated no evidence of prokaryotic or eukaryotic microbial infection within tissues of asteroids affected by SSWD. Asymptomatic adult *Pycnopodia helianthoides* were collected from several sites in Puget Sound, Washington, in January–April 2014 before disease occurrence at the collection sites. Animals were placed in separate 10-gallon glass aquaria with sand-filtered and UV-treated flow-through seawater on separate draw lines (i.e., seawater was not recirculated between aquaria; US Geological Survey Marrowstone Laboratory) and held at ambient temperature (8–9 °C). Viral challenges were performed with homogenates prepared from symptomatic animals. Tissues from symptomatic asteroids were homogenized in 10 mL of seawater from the aquarium housing the symptomatic animal. The tissue homogenate was initially centrifuged at 1,000 × *g* for 5 min at 4 °C to remove large debris before being split into two 5-mL aliquots. One aliquot was boiled for 7 min to serve as a control before both heat-treated (control) and non–heat-treated (virus exposed) homogenates were serially syringe-filtered through 1-μm pore size polycarbonate and 0.22-μm pore size polyethersulfone filters, resulting in a virus-sized inoculum. Each asteroid was injected with 0.5 mL of either control (i.e., heat-treated) or viral inocula (0.5 mL) into the coelomic cavity. After injection, animals were observed every morning and evening for SSWD signs.

The animals inoculated with virus-sized material showed disease signs after 10–17 d whereas control (heat-treated inoculum) individuals did not develop SSWD signs (Fig. 2). From one of the virus-exposed animals showing SSWD signs in the first challenge, we again isolated virus-sized material to challenge a new set of asymptomatic animals. This second set of inoculated individuals had disease signs after 8–17 d (and again no control animals that received heat-treated inoculum developed SSWD signs). These experiments demonstrate that the disease is transmissible from symptomatic to asymptomatic individuals and that the pathogenic agent is virus-sized (i.e., <200 nm in diameter).

Investigation of Viral Agents in SSWD-Affected Tissues

We sought to identify candidate viruses in inoculum by conducting metagenomic surveys to compare viral consortia inhabiting asymptomatic and SSWD-affected tissues. Tissue samples (~1-cm cross-section of a ray including body wall, epidermis, pyloric caeca, and gonad) were excised from 28 specimens (Tables S2–S5) with sterilized dissecting scissors and placed into sterile 50-mL plastic tubes. Viral metagenomes (i.e., metaviromes) were then prepared and analyzed following Gudenkauf et al. (16) (*SI Text*). All sequences have been deposited in GenBank under BioProject accession no. PRJNA253121.

Metaviromic analysis indicated a greater prevalence of parvovirus-like sequences in symptomatic relative to asymptomatic asteroid homogenates (in 2 of 13 asymptomatic libraries and 7 of 15 symptomatic libraries). Global assembly of all viral metagenomes (n = 28 libraries, representing 5×10^7 sequences and 1×10^{10} nt of information) resulted in assembly of a near-complete densovirus (*Parvoviridae*) genome, which we have named

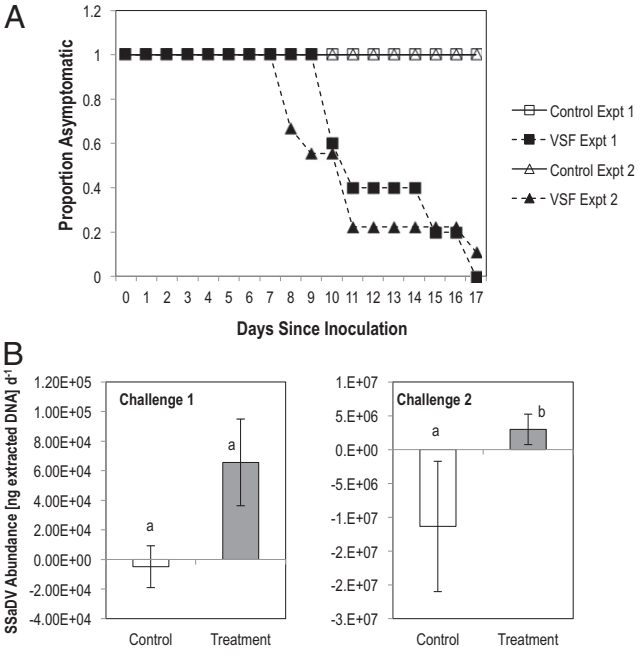

Fig. 2. (*A*) Proportion of stars remaining asymptomatic after inoculation with control (heat-killed) or virus-sized fraction (VSF) of asteroid homogenates in first (Expt 1) and second (Expt 2) challenge. Survival analysis (20) indicates that the time to lesion development differs among treatment and control groups (log-rank test: χ^2 = 18.6, df = 1, P = <0.0001), but there is no difference in time to development of lesions in the two experiments (log-rank test: χ^2 = 0.2, df = 1, P = 0.698) (*B*) Change in SSaDV load between initiation of viral challenge and termination of experiment (i.e., animal expiry in live challenge or euthanasia of control animals). Note difference in scale. Viral load was determined by quantitative PCR (qPCR) targeting the NS1 gene of the SSaDV genome. Different letters above bars indicate that the mean viral abundance change is significantly different (P < 0.05, two-tailed Wilcoxon signed-rank test to account for heteroskedasticity; Fisher's F-test P > 0.05). Error bars = SE.

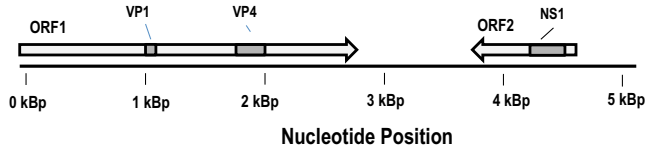

Fig. 3. Genome architecture of the sea star-associated densovirus (SSaDV).

sea star-associated densovirus (SSaDV) (Fig. 3). The SSaDV genome fragment bore architectural features similar to insect densoviruses but lacked their characteristic palindromic repeats. However, SSaDV is related to densoviruses in the Hawaiian sea urchins (Echinoidea) *Colobocentrotus atratus*, *Echinometra mathaei*, and *Tripneustes gratilla* (16) (Fig. 4), placing it near the only other known viruses of echinoderms. Purified preparations from three Northeastern Pacific asteroids (*Evasterias troschelii*, *P. helianthoides*, and *Pisaster ochraceus*) that had wide SSaDV representation in metagenomic libraries all contained non-enveloped icosohedral viral particles ~25 nm in size when negatively stained with uranyl acetate and viewed by transmission electron microscopy (TEM). The ultrastructure of these particles seems similar to other known viruses in the family *Parvoviridae* (Fig. 1). Comparison of viral metagenomes from symptomatic and asymptomatic asteroids did not reveal any other candidate viruses in tissue homogenates (see *SI Text* for details), confirming SSaDV as the sole virus associated with SSWD (Fig. S1).

To determine presence and load across a wider suite of individuals, quantitative PCR (TaqMan) primers were designed using Primer3 (4) specific to the nonstructural protein 1 (NS1) and viral gene product 4 (VP4) of SSaDV (*SI Text*). Quantitative PCR (qPCR) was performed following the approach of Hewson et al. (17), where template material comprised DNA extracted from small excisions of body wall or tube feet and where SSaDV copy number was divided by weight of tissue extracted.

In the experimental challenges with a virus-sized inoculum that elicited SSWD clinical signs, SSaDV load increased as disease signs appeared. In contrast, control asteroids receiving heat-killed virus-sized inoculum showed no SSWD signs, and SSaDV loads decreased over time. We attribute the initial low levels of SSaDV in the heat-treated qPCR to detection of heat-killed viral DNA that decayed after heat treatment (Fig. 2*B*). The inoculation experiments suggest that SSaDV is transmissible and can lead to wasting disease in exposed sea stars.

SSaDV Is Linked to Wasting Disease in Field Surveys

Due to the association of SSaDV with diseased asteroid tissues, we examined the incidence of SSaDV among symptomatic (n = 286 individuals) and asymptomatic (n = 49 individuals) asteroids of 14 species. Viral load (number of SSaDV copies detected per mg of tissue) and prevalence (i.e., percentage of samples where SSaDV was detected) were higher in symptomatic than in the asymptomatic animals in all three species where both symptomatic and asymptomatic animals were obtained (Fig. 5). However, the virus was present in both asymptomatic and symptomatic individuals in species where animals in both health states were sampled, including *P. ochraceus*, *P. helianthoides*, and *E. troschelii*. Because SSaDV detection varied by tissue type and location on each animal (Fig. S2), the single tissue sample taken from each individual likely led to some false negatives (in repeated sampling of body-wall tissues from symptomatic *P. ochraceus*, SSaDV was detected in 11–38% of samples). Due to the potential for these false negatives, it was not surprising that we observed SSaDV in some asymptomatic asteroids. Conversely, SSaDV in asymptomatic animals almost certainly represents viral presence before disease signs develop because we know from our inoculation experiment that signs can take 2 wk to progress after inoculation (or could represent viruses present on animal surfaces that had not yet gained entry to animal tissues).

Despite these procedural challenges, asteroids were more likely to be diseased if they had a high viral load (Fig. 6). In our statistical models involving viral load, we started with all factors and their first-order interaction terms. To focus our interpretation of model effects and increase power, we sequentially removed interaction terms that were not statistically significant (in order of their associated P value) and then did the same for main effects (this removal generally followed Akeike information criterion model selection). For the relationship between SSaDV load and disease, we used a logistic model of symptomatic vs. asymptomatic to evaluate the potential independent effects of SSaDV load, asteroid species, geography (San Diegan province or south of Point Conception vs. Oregonian province or north of Point Conception), and asteroid size (measured as arm circumference) in a sample of 107 symptomatic and asymptomatic *P. ochraceus*, *P. helianthoides*, and *E. troschelii* for which we had size measurements. The main significant predictive variable for being symptomatic was the SSaDV load [logistic regression, square root-transformed load of SSaDV, estimate = 0.0013 (0.0008 SE) chance of being symptomatic increasing with viral load, P = 0.006]. In addition, for a given viral load, asteroids from southern sites were more likely to be symptomatic [logistic regression, estimate = 0.95 (0.53 SE), P = 0.03] (Fig. 6). This result was consistent with analyses limited to *P. ochrace*us, which was the only species sampled in the North and South. However, neither asteroid size nor species had significant independent or interactive effects with the other factors. Given that viral load was the main predictor of disease, we then asked

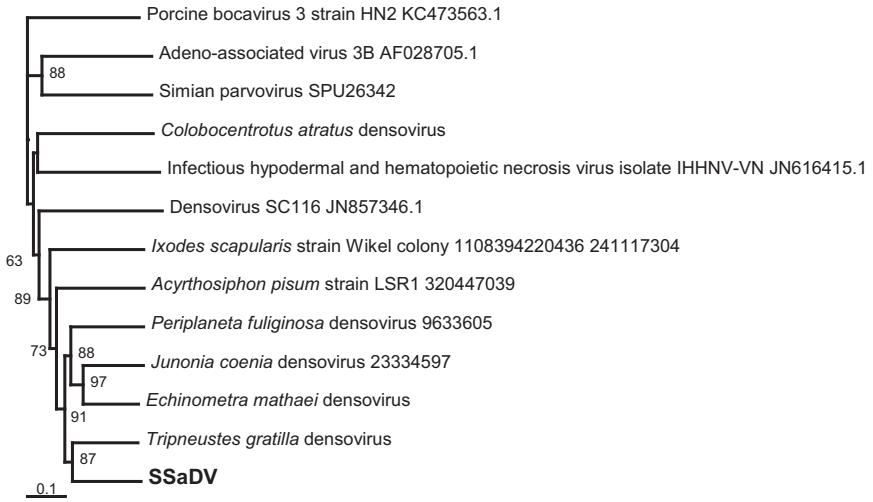

Fig. 4. Phylogenetic representation of the sea star-associated densovirus (SSaDV) NS1 capsid protein. The phylogenetic tree is based on an amino acid alignment performed by MUSCLE. The tree was constructed based on maximum-likelihood distance.

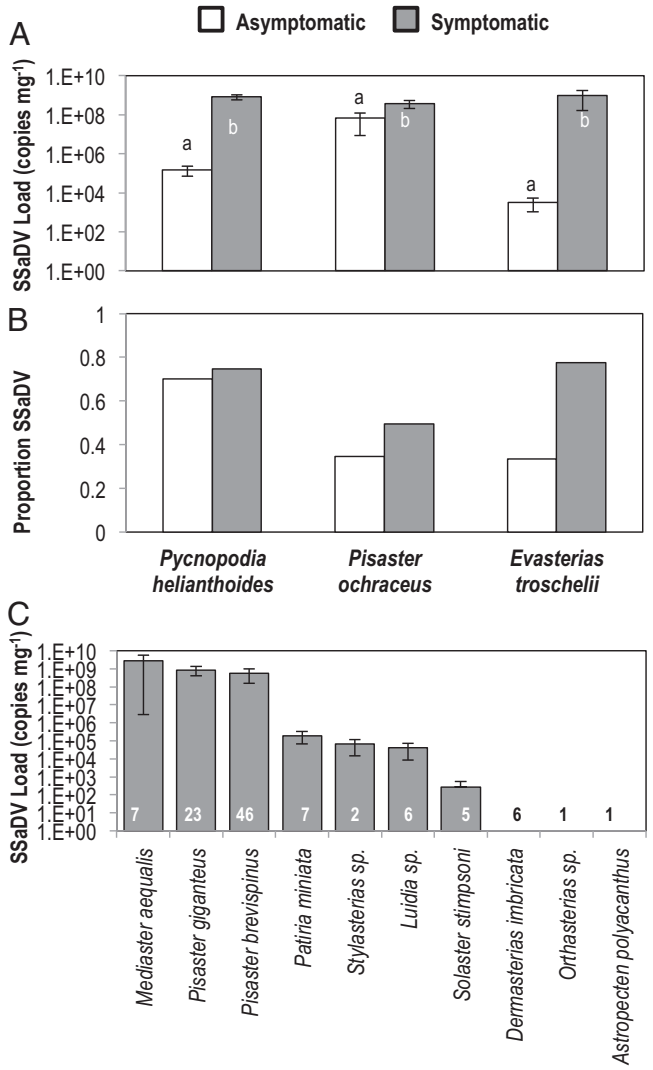

Fig. 5. (*A*) Mean viral load and (*B*) prevalence (i.e., proportion of SSaDV-positive individuals) (*B*) as determined by qPCR targeting the VP4 gene of the SSaDV genome. qPCR was applied to *P. helianthoides* ($n = 10$ asymptomatic and 79 symptomatic), *P. ochraceus* ($n = 26$ asymptomatic and 72 symptomatic), and *E. troschelii* ($n = 6$ asymptomatic and 31 symptomatic) whole-tissue DNA extracts. (*C*) SSaDV load in sympatric asteroid species. All stars except *Dermasterias imbricata, Orthasterias* sp., and *Astropecten polyacanthus* were symptomatic. The number of individuals tested is indicated for each species. Different letters within bars represent significant difference in the percentage of viral reads between asymptomatic and symptomatic asteroids ($P < 0.001$; df = 113 for *P. helianthoides*, df = 42 for *E. troschelii*, and df = 117 for *P. ochraceus*; data log-transformed and corrected for heteroskedasticity by $x/\sqrt{x}$; *t* test). The probability of being infected with the virus was higher in symptomatic asteroids. Logistic regression (generalized linear model with binomial distribution and logit link) comparing models with species and disease status and their interaction indicated that a model including species (likelihood ratio test: $\chi = 19.7$, df = 2; $P < 0.0001$) and disease status (likelihood ratio test: $\chi = 7.4$, df = 1; $P = 0.0065$) additively had the greatest support. This result indicates that viral prevalence differs among species and disease status, but the difference among disease status does not differ significantly among species (likelihood ratio test: $\chi = 2.50$, df = 1; $P = 0.29$). The odds ratios suggest that symptomatic stars are 3.2 times more likely to be virus-positive than asymptomatic stars. Error bars = SE.

what factors (species, geography, size) predicted viral load in 106 infected asteroids (from five species). A general linear model found a significant interaction between species and size ($P = 0.01$) due to a negative association between viral load and size in *P. helianthoides* (small individuals of *P. helianthoides* were more

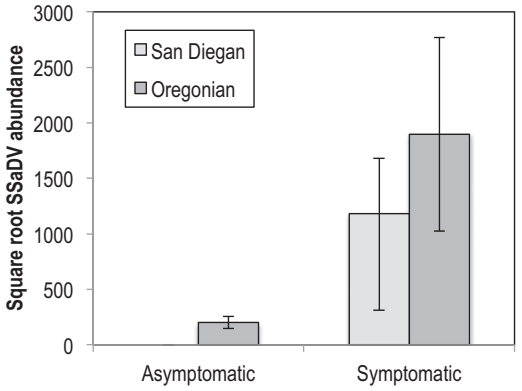

Fig. 6. Square root-transformed viral load in asymptomatic and symptomatic asteroids in San Diegan (i.e., south of Point Conception) and Oregonian (i.e., north of Point Conception) biogeographical provinces. For the relationship between SSaDV abundance and disease, we used a logistic model of symptomatic vs. asymptomatic to evaluate the potential independent effects of SSaDV abundance, sea star species, geography (San Diegan vs. Oregonian province), and sea-star size (measured as arm circumference) in the 107 *P. ochraceus*, *P. helianthoides*, and *E. troschelii* for which we had both size measurements and a mix of asymptomatic and symptomatic stars. The main significant predictive variable for being symptomatic was the abundance of SSaDV [logistic regression, square root-transformed count of SSaDV, estimate = 0.0013 (0.0008 SE) chance of being symptomatic increasing with viral count, $P = 0.006$]. Error bars = SE.

likely to have high viral counts), which was absent in the other four asteroid species. Therefore, our results provide strong evidence for a link between SSaDV and disease in wild asteroids.

To confirm the presence of viable SSaDV in host tissues, we performed quantitative reverse transcriptase PCR (qRT-PCR) on RNA extracted from symptomatic and asymptomatic individuals. SSaDV RNA, a proxy for viral presence and replication, was detected only in symptomatic *P. helianthoides* and *E. troschelii* and not in asymptomatic animals. However, SSaDV gene expression was observed in both symptomatic and asymptomatic *P. ochraceus*, suggesting that the host parasite dynamics may differ among species (Fig. 7).

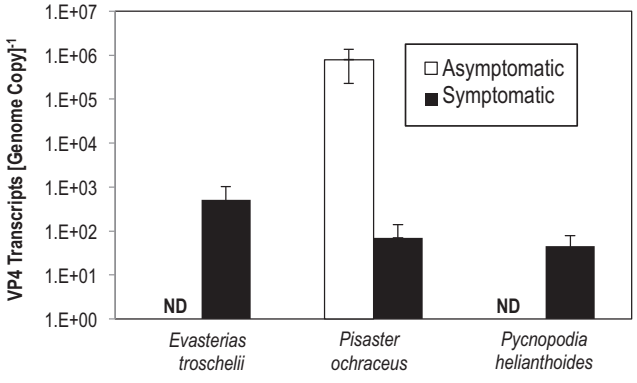

Fig. 7. Transcription of the SSaDV VP4 as assessed by qRT-PCR comparing asymptomatic and symptomatic tissues. qRT-PCR was performed on whole-tissue RNA extracts from *E. troschelii* ($n = 5$ asymptomatic and 5 symptomatic), *P. ochraceus* ($n = 5$ asymptomatic and 6 symptomatic), and *P. helianthoides* ($n = 10$ asymptomatic and 10 symptomatic), and normalized to quantities of SSaDV assessed by qPCR in cDNA extracts. Transcript levels were significantly higher in asymptomatic *P. ochraceus* than symptomatic individuals (Mann–Whitney *U* test; $P = 0.039$, df = 11). Error bars = SE.

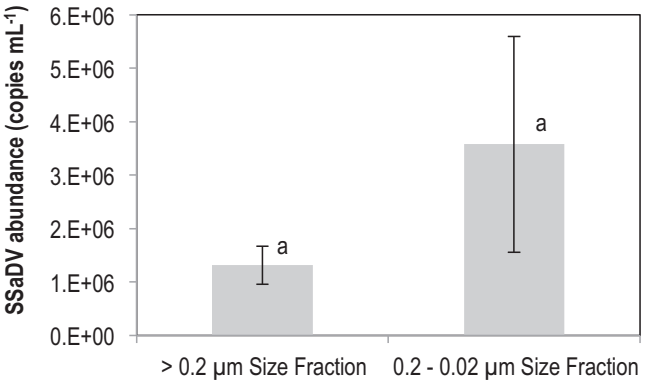

Fig. 8. Viral abundance in particle (i.e., >0.2 μm) and virioplankton (0.2–0.02 μm) size fractions of water collected at field sites, experimental incubations, and public aquaria. Viral abundance was determined by qPCR targeting the VP4 gene of the SSWDAV genome. Means were not significantly different.

SSaDV Present in Plankton, Sediments, and Nonasteroid Echinoderms

Given evidence for viral transmission between asteroids in the laboratory, we then sought to understand how SSaDV might move between wild host individuals and populations. To investigate whether uninfected asteroids could contact viruses free in the water, associated with suspended particles, or in sediments, we tested different environmental samples for SSaDV. SSaDV had its highest abundance in the virioplankton size fraction of the water (0.02–0.2 μm) and was present in the suspended particulate material size fraction > 0.2 μm (Fig. 8). SSaDV presence in particulate material is congruent with other observations of parvoviruses (16) and might represent viruses adsorbed to abiotic material, viruses in detrital particles from decayed animals, or viruses within larval asteroids. SSaDV was also found in sediments collected from public aquaria that had experienced SSWD several months earlier, and SSaDV was concentrated in sand filters used to treat incoming water and between aquaria (Fig. 9). Therefore, SSaDV might transmit between asteroids and among populations by mechanisms other than direct contact between diseased and healthy individuals, consistent with the observation that SSaDV-infected asteroids shed virus into the water column (Fig. S3). Water-column SSaDV transport helps explain how SSWD spreads among disjunct asteroid populations.

The SSWD epizootic has hit an alarming number of asteroid species in all shallow water habitats. Eight of 11 asteroid species sampled from SSWD areas contained SSaDV (Fig. 4). The broad range of species in which SSaDV was detected is unexpected

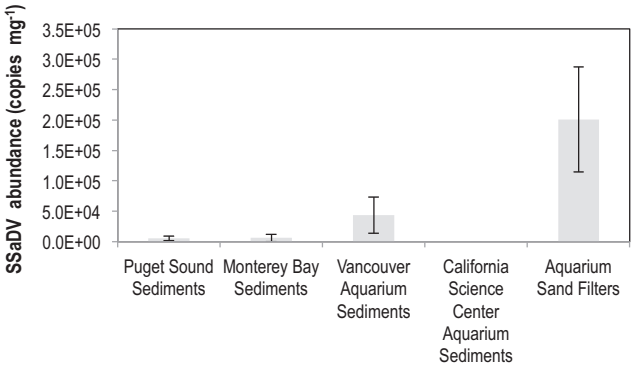

Fig. 9. Viral abundance in sediments from aquaria and field sites and in aquarium sand filters, as determined by qPCR targeting the VP4 gene of the SSaDV genome.

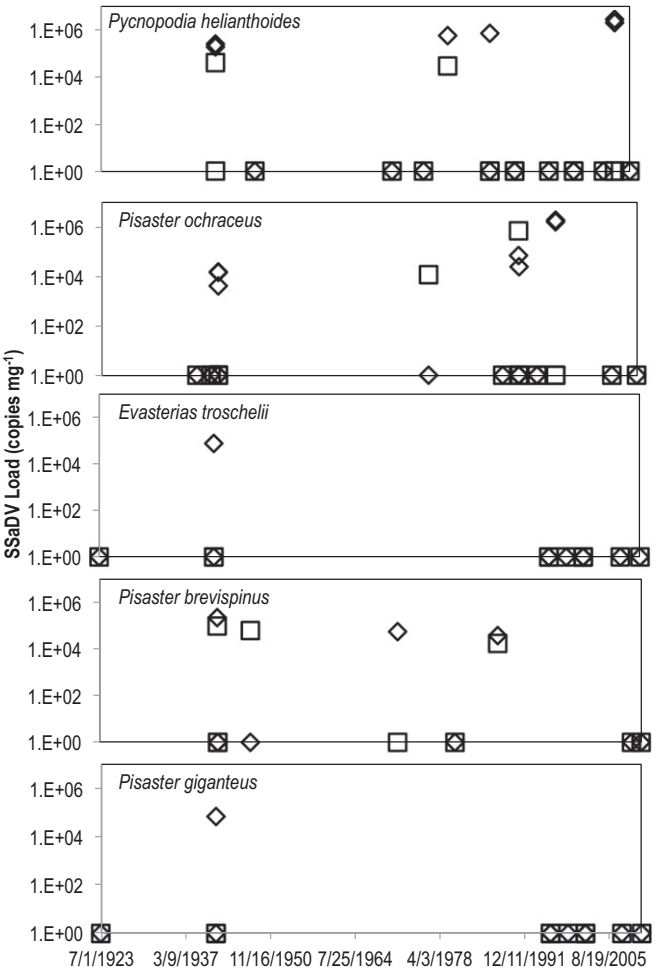

Fig. 10. Detection and load of SSaDV in ethanol-preserved museum specimens from 1923 to the present. SSaDV load was assessed by qPCR targeting the VP4 gene on the SSaDV genome and normalized to extracted tissue weight. We targeted both NS1 (□) and VP4 (◇) for this analysis because homologous viruses and recombination may have led to spurious results in old asteroids. Both NS1 and VP4 were found in 6 (of 67 tested) specimens from 1942, 1980, 1987, and 1991. We also detected large loads of either NS1 or VP4 in 16 asteroids. These results suggest that SSaDV or perhaps related densoviruses have been present in populations of several Northeastern Pacific Coast asteroid species, at least since 1942.

because most viruses infect a narrow range of host species. However, parvoviruses are known to infect across families, and variations in capsid protein secondary structure can result in variable host range (18). Parvoviruses gain entry to host cells via transferrin receptors, which are among the most highly expressed proteins in coelomic fluid (where, notably, it is found in coelomocytes, which are a major defense mechanism against cellular microbial infection) (19). It is also possible that receptors are shared between closely related sea-star species. This phenomenon is especially a possibility here because six of the eight species known to be affected by SSWD in which SSaDV was detected are within a single asteroid family (Asteriidae; the remaining two were within the Asterinidae) that may share common cell-surface features through which viruses may infect.

This broad host range inspired us to look for SSaDV in other Northeastern Pacific echinoderms. We observed SSaDV in sympatric, nonasteroid echinoderms, including echinoids (*Strongylocentrotus purpuratus* and *Dendraster excentricus*) and ophiuroids (Fig. S4). The impact of SSaDV on these taxa is unknown; however, the presence of the virus suggests that they could form a reservoir of SSaDV. If some echinoderms are

tolerant reservoirs of infection, it might help keep SSaDV in the system long after it extirpates less tolerant hosts, helping explain how SSWD can extirpate some host species while still persisting in an ecosystem. However, we cannot eliminate the possibility that detection of SSaDV in these species may represent free viruses attached to their surfaces or drawn into their water vascular systems, as opposed to those infecting tissues.

SSaDV Present in Asteroids 72 Years Ago

Its broad host range suggested that SSaDV could be associated with asteroid mortalities in other times and places. To better understand the geographic distribution of SSaDV, we studied Northwest Atlantic Coast asteroids with SSWD-like signs in 2012 and 2013. We used qPCR targeting two loci (VP4 and NS1) on the SSaDV genome to detect SSaDV from diseased *Asterias forbesii* from the Mystic Aquarium (Connecticut). Although we did not detect SSaDV gene transcription, the SSaDV DNA detected in 9 of 14 samples suggests that this virus might be present in other oceanic basins. Additionally, to investigate whether SSaDV was present in Northeast Pacific Coast asteroids before 2013, we tested for SSaDV in ethanol-preserved museum specimens collected between 1923 and 2010 at sites in British Columbia, Washington, Oregon, and California (Table S6). qPCR amplification detected SSaDV DNA (NS1 and VP4 loci) in asteroids that had been field-collected and preserved in July 1942, October 1980, September 1987, and July 1991 (Fig. 10). We also detected one locus in at least nine other individual asteroids, suggesting that viruses with homologous NS1 or VP4 were present in these populations, too. Therefore, SSaDV and related viruses might have infected asteroids on the North American West Coast decades before the current SSWD event.

If SSaDV is the cause of the current SSWD event, it is unclear why the virus did not elicit wide disease outbreaks in the past during periods in which it was detected; however, there are several possible reasons why the current SSWD event is broader and more intense than previous occurrences. SSaDV may have been present at lower prevalence for decades and only became an epidemic recently due to unmeasured environmental factors not present in previous years that affect animal susceptibility or enhance transmission. There are anecdotal reports from fishers and scuba divers that by 2012, the Salish Sea was severely overpopulated with adult *P. helianthoides*. Our finding of a strong relationship between size and SSaDV load, and anecdotal observations of SSWD commonly in adults but less so in juveniles in the field, suggest that the current event may be exacerbated by a large number of adult sea stars present in small bays and inlets. Because of its wide host range in the current event, we also speculate that variation of SSaDV (possibly by modification of capsid structure, as seen in other parvoviruses) (18) may have led to greater virulence. There remains much to be learned about the interactive effects of environmental transport, virulence, and environment on the dynamics of this disease.

Conclusions

In summary, SSWD has caused widespread and, until now, unexplained mass mortality in asteroids. SSWD spread has been most consistent with an infectious agent, which we suggest is a virus. Based on our observations, the densovirus, SSaDV, is the most likely virus involved in this disease. We base this statement on finding virus and disease transmission to healthy asteroids after exposure in two trials with virus-sized particles from diseased asteroids, finding replicating densovirus in diseased tissue, and an association between viral load and disease. Furthermore, our observation of SSaDV from 72 y ago suggests that, like many marine pathogens, SSaDV was already present in the environment before the outbreak. The detection of SSaDV in diverse echinoderm species and some sediments suggests a high potential for persistence in nonasteroid reservoirs. SSaDV is present in environmental samples, suggesting that it can spread outside of a host. However, it remains to be seen how infection with SSaDV kills asteroids, what the role is for other microbial agents associated with dying asteroids, what triggers outbreaks, and how asteroid mass mortalities will alter near-shore communities throughout the North American Pacific Coast. More generally, viral pathogens are poorly known for all noncommercial invertebrates yet may play an unrecognized, yet important, role in marine ecosystems.

ACKNOWLEDGMENTS. We thank Alice Nguyen, Armand Kuris, and Gretchen Hoffman [University of California (UC) Santa Barbara]; Elise Delaroque (UC Davis); Betsy Steele, Nathaniel Fletcher, Rani Gaddam, Melissa Redfield, Corianna Hume-Flannery, Sarah Sampson, Colin Gaylord, and Tristin McHugh (UC Santa Cruz); Steven Whittaker (National Parks Service); Stewart Johnson (Fisheries and Oceans Canada); Michael Garner (Northwest Zoopathology); Marina Krasnovid and Bryanda Wippel (University of Washington); Gene McKeen, Nate Schwarck, Jay Dimond, and Robert Boenish (Shannon Point Marine Center); Paul Hershberger [US Geological Survey (USGS) Marrowstone Island Laboratory]; Thierry Work (USGS); Sion Cahoon (Vancouver Aquarium); Kim Rotter (California Science Center); Allison Tuttle (Mystic Aquarium); Douglas Swanston and Neil McDaniel (Seacology Network); Shawn Larson and Bryan McNeil (Seattle Aquarium); Salvatore Frasca, Jr. (University of Connecticut); James Eaglesham, Sierra Helmann, Jacob Sangren (Cornell University); Rebecca Thurber (Oregon State University); and Laura James and Jan Kocian. Photographs in Fig. 1 *B* and *C* were provided by N. McDaniel. Research was supported by rapid response grants from the David R. Atkinson Center for a Sustainable Future (Cornell University), National Science Foundation Grant OCE-1401727 (to I.H. and B.M.), and Washington Sea Grant (to C.M.M. and B.M.).

1. Dungan ML, Miller TE, Thomson DA (1982) Catastrophic decline of a top carnivore in the Gulf of California rocky intertidal zone. *Science* 216(4549):989–991.
2. Eckert G, Engle JM, Kushner D (1999) Sea star disease and population declines at the Channel Islands. *Proceedings of the Fifth California Islands Symposium* (Minerals Management Service, Washington, DC), pp 390–393.
3. Bates AE, Hilton BJ, Harley CDG (2009) Effects of temperature, season and locality on wasting disease in the keystone predatory sea star *Pisaster ochraceus*. *Dis Aquat Organ* 86(3):245–251.
4. Zann L, Brodie J, Vuki V (1990) History and dynamics of the crown-of-thorns starfish *Acanthaster planci* (L) in the Suva Area, Fiji. *Coral Reefs* 9:135–144.
5. Pratchett MS (1999) An infectious disease in crown-of-thorns starfish on the Great Barrier Reef. *Coral Reefs* 18:272.
6. Tiffany WJ (1978) Mass mortality of *Luidia senegalensis* (Lamarck, 1816) on Captiva Island, Florida, with a note on its occurrence in Florida Gulf coastal waters. *Fla Sci* 41:63–64.
7. Sieling FW (1960) Mass mortality of the starfish, *Asterias forbesi*, on the Atlantic Coast of Maryland. *Chesap Sci* 1:73–74.
8. Lawrence JM (1996) Mass mortality of echinoderms from abiotic factors. *Echinoderm Studies*, eds Jangoux M, Lawrence JM (A.A. Balkema, Rotterdam), Vol 5, pp 103–137.
9. Thorpe JP, Spencer EL (2000) A mass stranding of the asteroid *Asterias rubens* on the Isle of Man. *J Mar Biol Assoc U K* 80:749–750.
10. Berger VY, Naumov AD (1996) Effects of salinity on the substrate attachability of the starfish *Asterias rubrens*. *Biologiya Morya* 22:99–101.
11. Scheibling RE, Hennigar AW (1997) Recurrent outbreaks of disease in sea urchins *Strongylocentrotus droebachiensis* in Nova Scotia: Evidence for a link with large-scale meteorologic and oceanographic events. *Mar Ecol Prog Ser* 152:155–165.
12. Staehli A, Schaerer R, Hoelzle K, Ribi G (2008) Temperature induced disease in the starfish *Astropecten jonstoni*. *Mar Biodivers Rec* 2:e78.
13. Suzuki G, Kai S, Yamashita H (2012) Mass stranding of crown-of-thorns starfish. *Coral Reefs* 31:821.
14. Sutton DC, Trott L, Reichelt JL, Lucas JS (1988) Assessment of bacterial pathogenesis in crown-of-thorns starfish, *Acanthaster planci*. *Proceedings of the Sixth International Coral Reef Symposium*, eds Choat JH, Barnes D, Borowitzka MA, Coll JC, Davies PJ, Flood P, Hatcher BG, Hopley D, Hutchings PA, Kinsey D, Orme GR, Pichon M, Sale PF, Sammarco P, Wallace CC, Wilkinson C, Wolanski E, Bellwood O (Australian Museum, Townsville, Australia), Vol. 2, pp. 171–176, contributed papers.
15. Rivera-Posada JA, Pratchett M, Cano-Gomez A, Arango-Gomez JD, Owens L (2011) Refined identification of Vibrio bacterial flora from *Acanthasther planci* based on biochemical profiling and analysis of housekeeping genes. *Dis Aquat Organ* 96(2):113–123.
16. Gudenkauf BM, Eaglesham JB, Aragundi WM, Hewson I (2014) Discovery of urchin-associated densoviruses (family Parvoviridae) in coastal waters of the Big Island, Hawaii. *J Gen Virol* 95(Pt 3):652–658.
17. Hewson I, et al. (2013) Metagenomic identification, seasonal dynamics and potential transmission mechanisms of a *Daphnia*- associated single-stranded DNA virus in two temperate lakes. *Limnol Oceanogr* 58:1605–1620.
18. Parker JS, Parrish CR (1997) Canine parvovirus host range is determined by the specific conformation of an additional region of the capsid. *J Virol* 71(12):9214–9222.
19. Harrington FE, Easton DP (1982) A putative precursor to the major yolk protein of the sea urchin. *Dev Biol* 94(2):505–508.
20. Harrington DP, Fleming TR (1982) A class of rank test procedures for censored survival data. *Biometrika* 69:553–566.

Supporting Information

Hewson et al. 10.1073/pnas.1416625111

Specimen Collection

Three hundred thirty-five specimens representing 14 species of asteroids were collected on the North American Pacific Coast between 19 September 2013 and 2 April 2014 (Table S1). Of these specimens, 138 individuals had been maintained in public aquaria (Monterey Bay Aquarium, Vancouver Aquarium, Long Marine Laboratory, Seattle Aquarium, Port Townsend Marine Science Center, and California Science Center), and the remainder were collected by hand from intertidal or subtidal habitats. Animals were classified as symptomatic and asymptomatic by contributors based on the presence (symptomatic) or absence (asymptomatic) of sea-star wasting disease (SSWD) signs, which included (*i*) loss of body turgor (deflation) and weakness, (*ii*) foci of epidermal pallor and tissue loss, (*iii*) sloughing of rays and/or rupture of the body wall with evisceration, and (*iv*) death. A purely visual approach to symptomatic versus asymptomatic categorization was necessary. More symptomatic (n = 286), were collected than asymptomatic individuals (n = 49). Among the species studied, the most numerous were *Pisaster ochraceus* (n = 88) and *Pycnopodia helianthoides* (n = 78), with fewer *Pisaster brevispinus* (n = 63), *Pisaster giganteus* (n = 35), *Evasterias troschelii* (n = 33), and *Patiria miniata* (n = 11), and all other species represented by <10 individuals. After collection, animals were either frozen at −20 °C immediately (for field samples) or chemically anesthetized (at some aquariums, with MS-222 or $MgCl_2$) and then frozen. Subsequently, specimens were then either sectioned into rays or sent as intact whole animals to the Department of Microbiology at Cornell University for further analysis.

Sampling Procedure and DNA Extraction

Asteroid specimens were thawed at room temperature and then sampled by removing an ∼2-mm-wide strip running from the aboral surface to the ambulacral groove of the animal (including tube feet, ampullae, and axial canal) with sterilized scissors and forceps. Samples were taken from the widest part of the ray of most specimens. Samples were placed into sterile Bead Basher tubes (Zymo Research) and frozen before nucleic acid extraction. To assess within-animal microbial detection variability, two symptomatic individuals of *P. ochraceus* obtained from Cuyler Harbor, San Miguel Island (Channel Islands), CA, were partitioned into 23 samples each, representing the distal tip, two midpoint samples, and body wall of the central disk between each of the five rays, in addition to samples of gonad, pyloric caeca/digestive tract, and tube feet. Each sample was ∼0.2 g and was placed into a sterile Bead Basher tube and frozen before analysis. All samples were weighed before nucleic acid extraction. Holobiont DNA was extracted from samples using the ZR Tissue and Insect Mini kit (Zymo Research) following the manufacturer's protocols.

Viral Metagenomics

Viral metagenomes (i.e., metaviromes) were prepared following Gudenkauf et al. (1). Tissue samples (∼1-cm cross-section of a ray including body wall, epidermis, pyloric caeca, and gonad) were excised from specimens (Tables S2–S5) with sterilized dissecting scissors and placed into sterile 50-mL Falcon tubes. Samples were then amended with 50 mL of 0.02 μm-filtered PBS and homogenized in a NutriBullet for 1 min. Tissue homogenates were centrifuged at 3,000 × g for 5 min, after which supernatants (5–50 mL) were sequentially filtered through GF/A (Whatman), and then through 0.2-μm polyethersulfone (PES) (VWR) filters. Filtered homogenates were amended with 10% (wt/vol) PEG-8000 and precipitated overnight at 4 °C. Samples were then centrifuged at 12,000 × g for 1 h at 4 °C to pellet high molecular weight organic matter (including viruses). The supernatant was decanted, and pellets were resuspended in 1 mL of nuclease-free water (Promega). Samples were then syringe-filtered through 0.2-μm PES filters and then amended with 0.2 volumes of chloroform and mixed. The mixtures were centrifuged for 10 min at 12,000 × g, and the supernatant was transferred to a new microcentrifuge tube. The purified DNA was treated with TURBO DNase (14 U), RNase One (20 U), and Benzonase nuclease (1 μL) and incubated at 37 °C for 2 h. At the conclusion of nuclease treatment, samples were amended with 20 μM EDTA. Viral DNA was extracted from 500-μL subsamples of nuclease-treated purified viral preparations using the ZR Viral DNA kit (Zymo Research), following the manufacturer's recommendations. Viral RNA was extracted using the RNA Mini Isolation kit (Zymo Research), and coextracted DNA was removed by using the DNA-free RNA kit (Zymo Research). After extraction, DNA was amplified using the WGA2 kit (Sigma Aldrich), and RNA was amplified using the WTA kit (Sigma Aldrich) before being submitted to the Cornell Core Biotechnology Resource Center Genomics Facility for sequencing using Illumina 2 × 200-bp HiSeq chemistry. All sequences have been deposited in GenBank under BioProject accession no. PRJNA253121.

For each library, sequence data were transferred to the CLC Genomics Workbench 4.0 where they were trimmed for quality (n < 2 ambiguous bases, sequences >200 bp or <200 bp were discarded) and assembled into contiguous sequences (minimum overlap 0.2 and identity 0.95). ORFs on contigs were determined using the GetORF algorithm (EMBOSS) (2). ORF sequences were analyzed by BLASTx comparison against the National Center for Biotechnology Information (NCBI) nonredundant (nr) protein database via the Community Cyberinfrastructure for Advanced Microbial Ecology Research and Analysis (CAMERA) (camera.calit2.net) (3). Contigs were phylogenetically annotated according to the top ORF hit (i.e., lowest E-value), where hits E > 10^{-3} were removed from further analysis. Recruitment information for each contig was then assigned to produce quantitative information on phylogenetic representation within each library.

Viral metagenomes contained between 5 × 10^5 and 4 × 10^6 reads, of which 41–80% assembled into contiguous sequences (Tables S2–S5). We focused analyses on contigs for annotation because the short length of sequence reads (200 bp) does not permit confidence in phylogenetic assignment. Between 2% and 60% of sequence reads assembling into contigs matched homologous proteins in the nonredundant database and could be assigned to a specific taxon based on their affiliation. Of these annotated contigs, the percentage of viral annotations was 0.02–25.45% of total sequence reads. The greatest proportion of viral reads was obtained in samples from *E. troschelii* from the Vancouver region (7.8–25.4% of reads) whereas the smallest was for *P. ochraceus* from Olympic National Park.

The majority of annotated reads within DNA viral metagenomic libraries were to Bacteria (45%) and Eukarya (39%) whereas viruses accounted for 0.1–68% (mean 15.3%). Among viral reads, most annotations were to bacteriophage (mean = 67%) and fewer to viruses of eukaryotic organisms (33%). In DNA metaviromic libraries, similarities to RNA viruses constituted only a small percentage (mean = 1.5%) of total viral reads

whereas, in RNA libraries, they constituted a much greater proportion (mean 43%).

Eukaryotic viral annotated reads in DNA libraries clustered primarily to phycodnaviruses and mimiviruses, both within the proposed family *Megaviridae*. Large representation of this viral family is likely a consequence of their extremely large size compared with other known viruses, or the presence of viruses that infect microscopic algae that may be present on animal surfaces or within digested food material or those present on the animal's exterior. In RNA libraries, Dicistroviruses constituted a large proportion of reads (41 ± 30% of symptomatic reads and 61 ± 9% of asymptomatic reads). Only two groups of viruses were disproportionately present in symptomatic compared with asymptomatic libraries: retroviruses and parvoviruses, the latter constituting a small fraction (2.23 ± 1.44% of total viral reads) (Fig. S1). Retroviral annotations are likely spurious because they were detected in DNA libraries (and have RNA as nucleic acids). With the exception of three samples (small *P. helianthoides* and *E. troschelii* from the Vancouver region and an asymptomatic *P. ochraceus* from Santa Cruz, CA), all hits to parvoviruses were from symptomatic asteroids ($n = 7$ libraries). Therefore, we targeted parvovirus-like viruses for further analyses.

Global assembly of all 28 metagenomes and screening for parvovirus-like fragments by BLASTn against a database of all known parvoviruses revealed the presence of a near-complete densovirus. The densovirus-like genome was not in our blank metavirome at any E-value by BLASTn analysis. We have previously observed densoviruses as a constituent of echinoid viral communities (1). The densovirus-like genome fragment was 5,050 nt and bore two ambisense ORFs that represent a well-characterized structural ORF (encoding VP4 and VP1) and nonstructural ORF (encoding NS1). We did not observe palindromic repeats at the distal ends of the genome fragment, suggesting that the contig does not represent a full viral genome. The VP1 protein (coat protein) was most similar to *Sibine fusca* densovirus (YP_006576514; E-value 2×10^{-17} by BLASTx) and the VP4 protein (major structural protein) was most similar to *Dysaphis plantaginea* densovirus (ACI01075; E-value 4×10^{-8} by BLASTx) whereas the NS1 protein was most homologous with *Periplaneta fuliginosa* densovirus (NP_051020; E-value 2×10^{-78} by BLASTx). Phylogenetic analysis based on the NS1 protein, which is a commonly used phylogenetic marker in studies of parvoviruses, indicated that the sea star-associated densovirus (SSaDV) is similar to a virus observed in the echinoid *Tripneustes gratilla*, but distinct from vertebrate parvoviruses and bocaviruses (Fig. 3).

Quantitative PCR of SSaDV

Quantitative PCR (TaqMan) primers were designed using Primer3 (4) specific to the nonstructural protein 1 (NS1; forward primer, 5′-ttaaggatcgggttcgtgtc-3′; reverse primer, 5′-tgcaagcggattaggtttct-3′; probe, 5′-tcaattggatgagtgcaccatttttga-3′; oligonucleotide standard, 5′-tttaaggatcgggttcgtgtcttcaattggatgagtgcaccatttttgaagaattatgataagaaacctaatccgcttgcag-3′) and viral gene product 4 (VP4; forward primer, 5′-ttgcattaattcctgctggt-3′; reverse primer, 5′-tgtaccaccagtgggatagc-3′; probe, 5′-tgatgtcatgcaaactgttgccaca-3′; oligonucleotide standard, 5-tttgcattaattcctgctggtagttacataaagtctgtatctattgatgtcatgcaaactgttgccacaactggctatcccactggtggtacaa-3′) of SSaDV. Primer specificity was checked by comparison of designed primers/probes and standards against the nonredundant database at NCBI by BLASTn. Quantitative PCR was conducted on asymptomatic and symptomatic asteroids in 25-μL reactions containing 1 X Universal Master Mix (Life Technologies), 200 pmol of each primer, and 1 μL of extracted DNA. Thermal cycling was performed in an ABI 7300 real-time thermal cycler. Thermal cycling comprised an initial denaturing step at 95 °C for 5 min, followed by 60 cycles of denaturing (95 °C for 30 s) and annealing (55.5 °C for 30 s). Each run of samples was accompanied by oligonucleotide standards over eight orders of magnitude and no-template controls. Detected gene-copy numbers were corrected for differences in extracted biomass by multiplying values by total extract volume and then dividing by the mass of asteroid tissue extracted. The practical detection limit of the VP4 primer set, based on the range of standards used in our study, was 2×10^2 copies per reaction, or 35 copies·mg^{-1} tissue. Quantitative PCR was performed on field-collected asteroids ($n = 339$) and for individual experiments as noted in subsequent sections. Viral loads were corrected for differences in the mass of holobiont extracted. Quantitative PCR inhibition was assessed in the first 80 samples analyzed by spiking samples with an internal oligonucleotide standard (10^4 copies per reaction) and comparing its cycle threshold value (Ct) to its respective standard run in a separate reaction. In these first 80 samples, no inhibition was observed.

Because of concerns that parvoviruses may be reagent contaminants, as observed in previous studies of parvovirus–circovirus hybrids (5), we rigorously interrogated a parallel "blank" viral metagenome but did not detect SSaDV. We also did not detect SSaDV in blank DNA extracts or in extracts of many asteroid specimens by PCR, strongly suggesting that SSaDV is not among recently described contaminants in molecular biology spin columns and reagents (5).

We sought to assess variability in viral load within individual animals and to determine whether nonlethal sampling of animals was feasible. Two *P. ochraceus* were sectioned into 22 tissue samples each, including body wall, arm tip, gonad, and digestive tract ($n = 20$), and nonlethal samples from tube feet ($n = 1$) and coelomic fluid ($n = 1$). We found considerable variability within and between both animals in SSaDV detectability (Fig. S2). SSaDVs were most consistently and with greatest abundance detected in tissues of samples of the interradial body wall of the central disk. Aboral and lateral body wall tissues were among the most variable tissues in which viral load was detected (SSaDV was detected in 11–38% of samples). Tube-feet samples demonstrated considerable variability in viral load, and variability was even greater in aboral and lateral body wall tissue of the arm. Overall, SSaDV was detected in 36–47% of tissue samples in symptomatic sea stars. These results suggest that single-location sampling of tissues describes potential viral load and prevalence, but SSaDV may in fact be present or more abundant elsewhere in animals. It is impractical to assay entire animals for every asteroid tested; therefore we feel that a combined sample of aboral and lateral body wall and tube feet (as used in this study for assessment of overall viral prevalence and load) adequately describes viral presence and abundance. Furthermore, both coelomic fluid and tube feet captured the presence of viruses and represent sublethal sampling that was used in later challenge experiments.

Quantitative Reverse Transcriptase PCR of SSaDV

To establish whether SSaDV was actively replicating, reverse-transcriptase quantitative PCR (qRT-PCR) was performed targeting the VP4 protein. RNA was extracted from *E. troschelii*, *P. ochraceus*, and *P. helianthoides* collected from several locations with the ZR RNA Mini Isolation Kit (Zymo Research). Extracted RNA was purified from coextracted DNA using the DNA-free RNA kit (Zymo Research). Total RNA was then converted to cDNA using SuperScript III (Life Technologies) before quantitative PCR analysis following the protocol above. For each sample, both cDNA and no-reverse transcriptase controls were quantified, and viral transcripts were corrected for no-RT controls and weight of sample extracted. Transcription of the structural gene was observed only in symptomatic *P. helianthoides* and *E. troschelii* compared with asymptomatic individuals. In *P. ochraceus,* transcription was significantly higher ($P < 0.05$, df = 10; *t* test) in asymptomatic than in symptomatic animals (Fig. 7).

Detection of SSaDV in Northwestern Atlantic Coast Samples

Similar SSWD-like symptoms were reported in Atlantic Coast asteroid populations between 2011 and 2013. Samples of apparently symptomatic *Asterias forbesii* from the Northwestern Atlantic Coast ($n = 15$) were obtained from the Mystic Aquarium. Samples were collected on 13 October 2012, 20 October 2012, 18 October 2013, 23 October 2013, 25 October 2013 ($n = 2$), 26 October 2013, and February 2014 ($n = 5$). Samples of asteroid tissues, similar to those from the Pacific Coast (described in *Sampling Procedure and DNA Extraction*), were collected, and DNA was extracted using the ZR Tissue and Insect kit (Zymo Research). Quantitative PCR targeting the NS1 and VP4 regions of SSaDV was performed on DNA extracts. SSaDV was detected in 9 of 15 samples, including all 3 samples from 2012, but only 2 of 5 samples from 2014. We also detected SSaDV by NS1 gene presence, which concurred with VP4 results in 3 asteroids (1 from 2012 and 2 from 2013). Therefore, the SSaDV detected in Pacific Coast asteroid samples was detected in asteroids from both the Atlantic Coast during the same time period of the Pacific Coast asteroid mortality event as well as in samples from 2012, which predates the disease event on the West Coast. The fact that some asteroids were positive only using the VP4 primers suggests that Atlantic asteroid tissues may have contained related, but not identical, densovirus genomes as well.

Longitudinal Study of SSaDV Dynamics

Eight asymptomatic small (~20-cm diameter) *P. helianthoides* were collected from Salsbury Point, Hood Canal in January 2014 and transported to a holding facility at USGS Marrowstone Laboratory before being shipped overnight to the Department of Microbiology at Cornell University. Three living animals were held overnight in a 20-L aquarium with juvenile (2-cm diameter) *P. helianthoides* from northern British Columbia (later found to have high loads of SSaDV) whereas the remainder were maintained in a second 20-L holding tank. After 1 d, the three animals that had cohabitated with juveniles were placed in the holding tank with the remaining five animals. Tube-foot clippings (~10 tube feet from each animal) were collected from each individual after 2 d, and load of SSaDV was determined by qPCR. At this time, the three asteroids that had cohabitated with juvenile asteroids were positive for SSaDV whereas the remaining five were negative. After 7 d, individual animals were placed in eight separate, 3.7-L aquaria in artificial seawater (Instant Ocean) at 8 °C on a 12-h light:dark cycle with continuous aeration and charcoal filtration. After the commencement of the experiment (where animals were housed individually), all seven asteroids had detectable abundances of SSaDV, suggesting that it had been transmitted from the infected asteroids. None of the animals fed on ~0.5 g of mussel tissue (obtained from a local supermarket) placed in each aquarium.

Coelomic fluid samples were obtained from each animal by drawing ~50 μL of fluid using a 3-mL syringe fitted with a 25 G needle from the perivisceral coelom. Coelomic fluid samples were obtained every 48 h until the animals died (after 11–14 d) or were euthanized by freezing. Aquarium water samples (50 mL syringe-filtered serially through 0.2- and 0.02-μm filters) were collected at 0 d, 4 d, and 10 d. Animals were killed by freezing at −80 °C after 14 d, and tissue samples were collected from arms per field samples. DNA was extracted from tissue, water column, and coelomic fluid samples. Over 14 d after isolation, coelomic fluid loads of SSaDV increased by over two orders of magnitude (Fig. S6). We also investigated the abundance of free-living viruses after 7 d and 14 d in aquaria. SSaDV abundance in the >0.02-μm-size fraction increased over time. Finally, we assessed viral load in euthanized animal tissues after 14 d. Tissue viral loads were similar to coelomic fluid loads in all animals. These results demonstrate that SSaDV abundance increases in animals over time during containment and that release/shedding of viruses occurs between 0 d and 14 d incubation. Further, these results show agreement between coelomic fluid viral loads and viral loads in tissues after 14 d.

Viral-Challenge Experiments

Asymptomatic adult *P. helianthoides* (size, 153 ± 35 cm average radius) were collected from Dabob Bay, Hood Canal, WA; Port Hadlock, Puget Sound, WA; San Juan Island, Straight of George, WA; and Langley, Puget Sound, WA, January–April 2014 before disease occurrence at each site. Animals were observed for disease signs until each experiment was started, and tissue samples (tube feet) were collected at the beginning of experiments to determine initial SSaDV load. Viral challenges were performed with homogenates prepared from symptomatic animals. Each asteroid was treated with either control or viral inocula (0.5 mL) by injection into the coelomic cavity.

Pairs of animals of similar size that were collected at the same time and location were haphazardly assigned to either the control or experimental treatment group. After injection, animals were observed every morning and evening. They were fed manila clams every 3 d. Tissue samples (tube feet) were collected for determination of SSaDV load after 8 d incubation and when the animals were killed. Early signs of disease (arm curling) were noted, and animals were killed when signs of tissue degradation were evident (lesions, arm amputation). Two experiments were conducted. In the first experiment, five control and five viral inocula (<0.02-μm size fraction) were performed. To further explore whether virus-sized particles might be the causative agent for disease, a second challenge was performed, where tissue from three animals that developed disease signs during the first experiment was used to make the control and viral inoculum for a second passage. The second experiment comprised 10 control and 10 viral inoculum-treated asteroids.

Survey of Museum Specimens

To investigate the historical presence of SSaDV in asteroids, we examined its occurrence in museum specimens collected from the Northeastern Pacific Coast between 1923 and 2010 (Table S6). Samples comprised tube feet excised from ethanol-preserved specimens in the echinoderm collection of the Natural History Museum of Los Angeles County. Specimens were selected to represent a range of species, dates, and geographic locations. Approximately 10 tube feet were removed from each specimen using sterile forceps and dissection scissors. The tube-foot samples were placed into sterile Bead Basher (Zymo) tubes and transported at room temperature to the laboratory at Cornell University. DNA was extracted from tube-foot samples using the Tissue and Insect Mini Kit (Zymo Research) according to the manufacturer's protocols. Viral presence and load were determined in samples by qPCR targeting the NS1 and VP4 regions of the SSaDV genome.

Survey of Nonasteroid Samples

The presence of SSaDV was examined in environmental reservoirs, including sediments, virioplankton (0.2 μm > virioplankton > 0.02 μm), bacterioplankton and larger particles (>0.2 μm), and sand filters in aquaria. DNA was extracted from subsamples (~200 mg) of sediment and sand-filter samples using the ZR Soil DNA kit (Zymo Research) according to the manufacturer's recommendations. DNA from water-column samples (which had been filtered onto 0.2-μm PES and 0.02-μm Anotop filters) was extracted using the ZR Viral DNA kit with modifications for filters (6).

SSaDV was detected in almost all sediments tested (13 of 15 samples) and was present in all sand-filter samples tested (Fig. 9). The abundance of SSaDV in sediments was generally lower than in sand filters; however, there was no difference between sediments at field sites and those from public aquaria. Interestingly, SSaDV was present in sediments at the bottom of

two aquaria that had previously housed symptomatic asteroids (samples were taken ~2 mo after asteroid death), but SSaDV was not detected in sediments at the bottom of the California Science Center kelp tank, which had never housed symptomatic asteroids. In plankton, SSaDV was found in the 0.02-μm-size fraction at abundances threefold higher than in the 0.2-μm-size fraction (Fig. 8). Mean SSaDV overall (2.5×10^6 copies·mL^{-1}) represents ~1–5% of virioplankton, which is higher than previous reports of metazoan viruses in plankton (6).

In addition to abiotic samples, the presence of SSaDV was assayed in specimens of ophiuroids and echinoids collected from public aquaria and in the field. DNA was extracted from tissue samples (for ophiuroids, a 0.5-cm section of arm; for echinoids, a 200-mg sample of gonad) using the ZR Tissue and Insect DNA kit (Zymo Research).

SSaDV was detected in 7 of 11 *Strongylocentrotus purpuratus*, in the single *Dendraster excentricus* from Bellingham, and in 2 of 6 ophiuroid specimens (Order Ophiurida) and not in the single specimen of *Gorgonocephalus eucnemis* (Order Euryalida) (Fig. S4). Although mortality of echinoids and ophiuroids has been reported in the field, we did not attempt to link disease in nonasteroids to microbiome composition.

1. Gudenkauf BM, Eaglesham JB, Aragundi WM, Hewson I (2014) Discovery of urchin-associated densoviruses (family Parvoviridae) in coastal waters of the Big Island, Hawaii. *J Gen Virol* 95(Pt 3):652–658.
2. Rice P, Longden I, Bleasby A (2000) EMBOSS: The European Molecular Biology Open Software Suite. *Trends Genet* 16(6):276–277.
3. Sun S, et al. (2011) Community cyberinfrastructure for Advanced Microbial Ecology Research and Analysis: The CAMERA resource. *Nucleic Acids Res* 39(Database issue): D546–D551.
4. Rozen S, Skaletsky H (2000) *Bioinformatics Methods and Protocols*, eds Krawertz S, Misener S (Humana, Totowa, NJ), pp 365–386.
5. Naccache SN, et al. (2013) The perils of pathogen discovery: Origin of a novel parvovirus-like hybrid genome traced to nucleic acid extraction spin columns. *J Virol* 87(22): 11966–11977.
6. Hewson I, et al. (2012) Temporal dynamics and decay of putatively allochthonous and autochthonous viral genotypes in contrasting freshwater lakes. *Appl Environ Microbiol* 78(18):6583–6591.

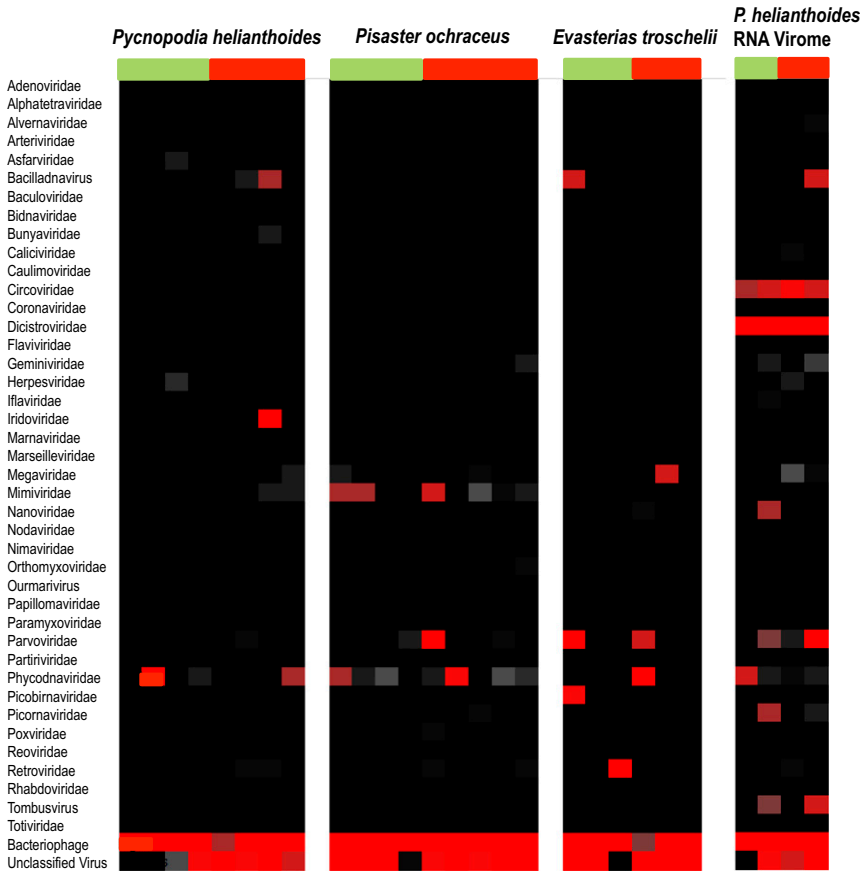

Fig. S1. Heat-map representation of viral families present in asymptomatic (green) and symptomatic (red) asteroid tissues. Annotation is based on the percentage of reads of total libraries and on BLASTx against the nonredundant database at NCBI. Each column represents a replicate metagenomic library.

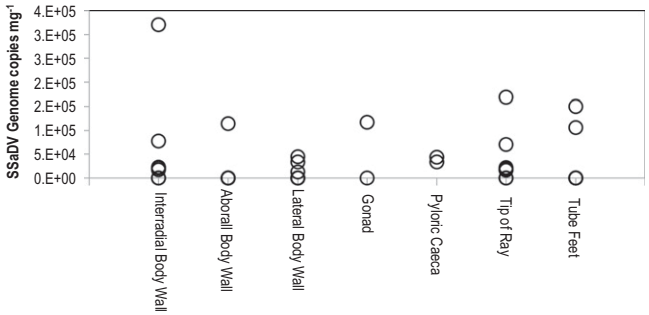

Fig. S2. Within-animal variability in SSaDV load as assessed by qPCR targeting the VP4 gene. Each circle indicates the load of SSaDV detected by qPCR in each tissue type. Analysis was performed on two symptomatic *P. ochraceus* obtained from Cuyler Harbor, San Miguel Island (Channel Islands), CA, on 18 January 2014. SSaDV was detected in 36% and 47% of subsamples from the symptomatic star, but detection varied from 11–77% of subsamples tested in individual tissues. Body-wall tissues, which were used to detect prevalence and load of SSaDV in field populations, yielded positive detection in only 11–38% of samples, suggesting the possibility of false negatives in the survey.

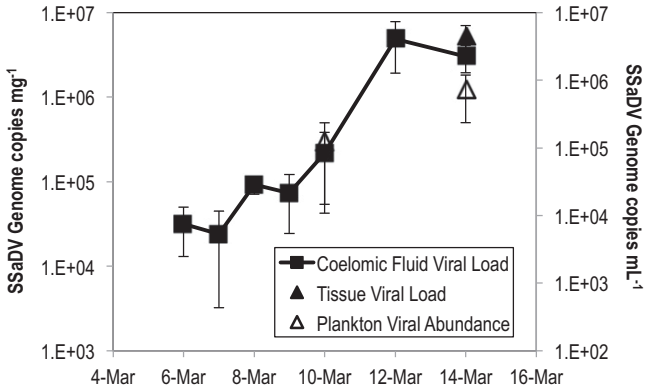

Fig. S3. Viral load in coelomic fluid and tissues and abundance in plankton during longitudinal study of SSaDV dynamics in aquaria. SSaDV load and abundance were determined by qPCR targeting the VP4 gene on the SSaDV genome. For coelomic-fluid load, viral abundance was normalized to total volume of coelomic fluid extracted.

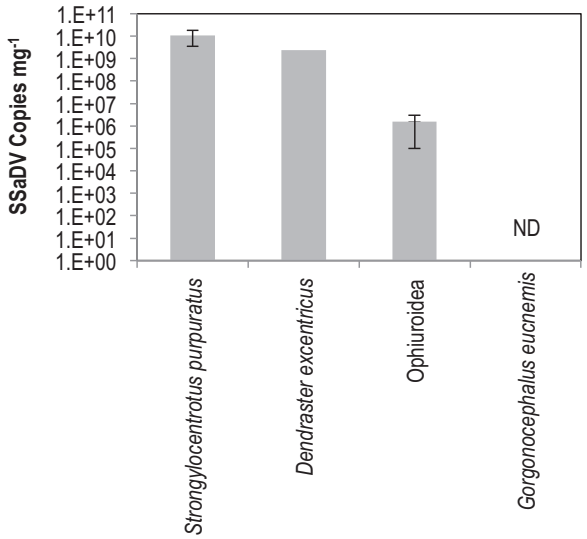

Fig. S4. Viral load in non-Asteroidea echinoderms as detected by qPCR targeting the VP4 gene on the SSaDV genome.

Table S1. Numbers of individual asteroids analyzed

Species	Location	Asymptomatic	Symptomatic
Patiria miniata	California Science Center (A)	0	4
	Monterey Bay Aquarium (A)	0	5
	Long Marine Laboratory/UCSC (A)	0	1
	Vancouver Aquarium (A)	0	1
Astrometis sertulifera	California Science Center (A)	0	4
Astropecten polyacanthus	California Science Center (A)	1	0
Dermasterias imbricata	Friday Harbor Laboratories (F)	1	0
	Santa Barbara, CA (F)	3	0
	Seattle Aquarium (A)	1	0
Evasterias troschelii	Port Hardy, British Columbia (F)	0	3
	Vancouver, British Columbia (F)	2	3
	Friday Harbor Laboratories (F)	3	2
	Olympic National Park (F)	0	2
	Dabob Bay, Hood Canal (F)	0	4
	Port Townsend, Puget Sound (A)	0	1
	Mukilteo, Puget Sound (F)	0	5
	Seattle Aquarium (A)	1	6
	Vancouver Aquarium (A)	0	1
Luidia foliolata	Vancouver Aquarium (A)	0	2
	Seattle Aquarium (A)	0	4
Mediaster aequalis	Vancouver Aquarium (A)	0	2
	Monterey Bay Aquarium (A)	0	1
Orthasterias sp.	Seattle Aquarium (A)	0	1
Pisaster brevispinus	Vancouver, British Columbia (F)	0	1
	Bainbridge Island, Puget Sound (F)	0	2
	Dabob Bay, Hood Canal (F)	0	1
	Carpinteria, CA (F)	0	28
	Seattle Aquarium (A)	0	4
	Vancouver Aquarium (A)	0	27
Pisaster giganteus	Santa Cruz, CA (F)	0	9
	Carpinteria, CA (F)	0	5
	Santa Barbara, CA (F)	0	4
	California Science Center (A)	0	6
	Monterey Bay Aquarium (A)	0	2
	Seattle Aquarium (A)	1	8
Pisaster ochraceus	Vancouver, British Columbia (F)	0	1
	Olympic National Park (F)	15	19
	Friday Harbor Laboratories (F)	0	5
	Dabob Bay, Puget Sound (F)	0	8
	Alki, WA (F)	0	4
	Mukilteo, WA (F)	0	4
	Santa Cruz, CA (F)	10	15
	San Miguel Island, Channel Islands (F)	0	2
	California Science Center (A)	0	5
Pycnopodia helianthoides	Vancouver, British Columbia (F)	5	2
	Friday Harbor Laboratories (F)	0	18
	Olympic National Park (F)	0	2
	Whidbey Island, WA (F)	0	4
	Dabob Bay, Hood Canal (F)	0	1
	Santa Barbara, CA (F)	0	2
	Vancouver Aquarium (A)	1	20
	Seattle Aquarium (A)	5	16
	Monterey Bay Aquarium (A)	0	2
Solaster stimpsoni	Friday Harbor Laboratories (F)	0	5
Stylasterias forreri	Vancouver Aquarium (A)	0	2
Total Individuals		49	286

A, aquarium; F, field site.

Table S2. Characteristics of viral metagenomes sequenced as part of this study: V1–V8

Library name	V1	V2	V3	V4	V5	V6	V7	V8
Species	*Dermasterias imbricata*	*Solaster stimpsoni*	*Solaster stimpsoni*	*Evasterias troschelii*	*Pycnopodia helianthoides*	*Evasterias troschelii*	*Pycnopodia helianthoides*	*Pycnopodia helianthoides*
S/A	S	S	S	S	S	A	A	A
Location	Friday Harbor Lab	Friday Harbor Lab	Friday Harbor Lab	Friday Harbor Lab	Friday Harbor Lab	Friday Harbor Lab	Friday Harbor Lab	Croker Island, Indian Arm, Burrard Inlet
Date	13 Oct 2013	10 Oct 2013	11 Oct 2013	7 Oct 2013	11 Oct 2013	8 Oct 2013	8 Oct 2013	29 Oct 2013
RNA/DNA	DNA	DNA	DNA	DNA	DNA	DNA	DNA	DNA
No. of total reads	1,007,652	3,500,172	1,455,342	1,951,510	3,233,230	1,432,820	678,554	1,924,530
No. of reads assembling into contigs	649,193	2,816,306	1,093,359	1,143,245	1,706,209	949,592	395,484	1,316,347
No. of contigs	4,867	3,162	1,846	2,429	1,697	3,416	1,435	9,739
Avg contig length, bp	457	334	335	390	458	368	475	403
No. of annotated reads	80,229	184,712	105,821	307,056	265,216	540,673	152,439	285,639
No. of viral reads	29,025	5,244	33,776	19,204	18,931	973	374	5,293

S, symptomatic; A, asymptomatic.

Table S3. Characteristics of viral metagenomes sequenced as part of this study: V9–V16

Library name	V9	V10	V11	V12	V13	V14	V15	V16
Species	*Pisaster ochraceus*	*Pycnopodia helianthoides*	*Pycnopodia helianthoides*	*Pycnopodia helianthoides*	*Pycnopodia helianthoides*	*Pisaster ochraceus*	*Pisaster ochraceus*	*Pisaster ochraceus*
S/A	A	A	A	S	S	A	A	S
Location	Cates Park Reef, Burrard Inlet	Seattle Aquarium	Seattle Aquarium	Seattle Aquarium	Seattle Aquarium	Olympic National Park	Olympic National Park	Olympic National Park
Date	29 Oct 2013	26 Oct 2013	26 Oct 2013	26 Oct 2013	26 Oct 2013	19 Sep 2013	19 Sep 2013	19 Sep 2013
RNA/DNA	DNA	DNA	DNA	DNA	DNA	DNA	DNA	DNA
No. of total reads	1,186,824	2,783,328	1,468,056	3,284,842	1,626,722	1,263,860	1,231,402	799,760
No. of reads assembling into contigs	753,998	1,379,247	830,906	2,234,614	1,045,925	829,203	746,472	464,081
No. of contigs	3,913	2,175	2,404	8,923	3,977	9,578	5,932	2,427
Avg contig length, bp	405	442	444	391	423	412	424	384
No. of annotated reads	154,622	517,622	160,642	486,945	488,751	89,716	98,735	46,038
No. of viral reads	10,062	10,686	19,715	6,544	38,382	3,752	12,078	71

S, symptomatic; A, asymptomatic.

Table S4. Characteristics of viral metagenomes sequenced as part of this study: V17–V24

Library name	V17	V18	V19	V20	V21	V22	V23	V24
Species	*Pisaster ochraceus*	*Pisaster ochraceus*	*Pisaster ochraceus*	*Pisaster ochraceus*	*Pisaster ochraceus*	*Pycnopodia helianthoides*	*Pycnopodia helianthoides*	*Evasterias troschelii*
S/A	S	S	S	A	A	S	A	S
Location	Olympic National Park	Santa Cruz	Santa Cruz	Santa Cruz	Santa Cruz	Gower Point	Gower Point	Cape Roger Curtis
Date	19 Sep 2013	8 Oct 2013	8 Oct 2013	8 Oct 2013	8 Oct 2013	17 Oct 2013	17 Oct 2013	17 Oct 2013
RNA/DNA	DNA	DNA	DNA	DNA	DNA	DNA	DNA	DNA
No. of total reads	1,255,558	1,235,128	1,503,372	1,928,276	1,136,824	1,407,560	1,806,572	2,615,580
No. of reads assembling into contigs	717,005	628,937	968,409	1,266,256	700,500	889,083	1,003,950	1,635,326
No. of contigs	4,238	4,248	5,195	8,241	2,615	3,264	1,365	1,234
Avg contig length, bp	390	432	433	421	383	399	458	593
No. of annotated reads	55,121	59,786	282,022	27,979	36,010	200,118	350,457	588,337
No. of viral reads	1,795	6,583	58,070	3,629	3,728	4,321	434	127,407

S, symptomatic; A, asymptomatic.

Table S5. Characteristics of viral metagenomes sequenced as part of this study: V25–V33

Library name	V25	V26	V27	V28	V30	V31	V32	V33
Species	*Evasterias troscheliii*	*Evasterias troschelii*	*Evasterias troscheliii*	*Asterina miniata*	*Pycnopodia helianthoides*	*Pycnopodia helianthoides*	*Pycnopodia helianthoides*	*Pycnopodia helianthoides*
S/A	S	A	A	S	A	A	S	S
Location	Cape Roger Curtis	Cape Roger Curtis	Cape Roger Curtis	Vancouver Aquarium	Seattle Aquarium	Seattle Aquarium	Seattle Aquarium	Seattle Aquarium
Date	17 Oct 2013	17 Oct 2013	17 Oct 2013	17 Oct 2013	26 Oct 2013	26 Oct 2013	26 Oct 2013	26 Oct 2013
RNA/DNA	DNA	DNA	DNA	DNA	RNA	RNA	RNA	RNA
No. of total reads	1,069,772	645,446	461,852	1,047,486	2,098,860	1,590,274	634,154	1,449,257
No. of reads assembling into contigs	547,055	297,307	191,102	477,486	1,014,703	724,150	283,171	850,072
No. of contigs	2,231	564	337	1,082	25,017	11,066	9,809	10,431
Avg contig length, bp	665	631	615	685	718	687	702	834
No. of annotated reads	253,085	41,691	115,094	83,349	317,421	229,370	125,939	427,794
No. of viral reads	139,216	28,465	46,917	25,284	5,359	99,312	20,436	102,749

S, symptomatic; A, asymptomatic.

Table S6. Natural History Museum of Los Angeles County specimens analyzed for detection of SSaDV

Species	Date	Location	Depth, m	Museum catalog no.
Evasterias troschelii	28 Jun 1942	S side of Sunset Bay, Coos Co, OR	Inter.	LACM 1942-22.18
Evasterias troschelii	28 Jun 1942	S side of Sunset Bay, Coos Co, OR	Inter.	LACM 1942-22.18
Evasterias troschelii	29 Jul 1942	Reef and bight at Cape Arago Lighthouse, Coos Co, OR	Inter.	LACM 1942-48.18
Evasterias troschelii	29 Jul 1942	Reef and bight at Cape Arago Lighthouse, Coos Co, OR	Inter.	LACM 1942-48.18
Evasterias troschelii	29 Jul 1942	Reef and bight at Cape Arago Lighthouse, Coos Co, OR	Inter.	LACM 1942-48.18
Evasterias troschelii	29 Jul 1942	Reef and bight at Cape Arago Lighthouse, Coos Co, OR	Inter.	LACM 1942-48.18
Evasterias troschelii	29 Jul 1942	Reef and bight at Cape Arago Lighthouse, Coos Co, OR	Inter.	LACM 1942-48.18
Evasterias troschelii	26 Jul 1971	Arena Cove, Mendocino Co, CA	12	LACM-1971-103.4
Pisaster brevispinus	7–10 Aug 1942	Depoe Bay, OR	110–135	LACM 1942-55.6
Pisaster brevispinus	7–10 Aug 1942	Depoe Bay, OR	110–135	LACM 1942-55.6
Pisaster ochraceus	30 Oct 1947	Big Rock Beach, CA	Inter.	LACM 1947-25.9
Pisaster brevispinus	30 Jul 1971	Humboldt Co, CA	8–15	LACM 1971-109.8
Pisaster brevispinus	24–26 Oct 1980	Morro Bay, CA	Inter.	LACM 80-174.1
Pisaster brevispinus	6 Sep 1987	Wickaninish Bay, Vancouver Island, British Columbia	45	LACM 87-114.9
Pisaster brevispinus	28 Feb 2009	Palos Verdes, CA	15–18	LACM 2009-12.1
Pisaster brevispinus	2 Jul 1942	Douglas Co., OR	48–106	LACM 1942-30.5
Pisaster giganteus capitatus	31 Jul 1923	Point Fermin, CA	n/a	LACM 1923-6.2
Pisaster giganteus capitatus	13 Feb 1942	Palos Verdes, CA	Inter.	LACM 1942-4.17
Pisaster giganteus capitatus	13 Feb 1942	Palos Verdes, CA	Inter.	LACM 1942-4.17
Pisaster giganteus	17 Feb 1996	Corona del Mar, CA	Inter.	LACM 96-1.7
Pisaster giganteus	19 Feb 1996	False Point, La Jolla, CA	Inter.	LACM 96-2.3
Pisaster giganteus	18 Dec 1998	Cayucos, Morro Bay, CA	Inter.	LACM 98-89.4
Pisaster giganteus	22 Sep 2001	San Clemente Island, CA	17	LACM 2001-58.1
Pisaster giganteus	22 Sep 2001	San Clemente Island, CA	15	LACM 2001-59.1
Pisaster giganteus	22 Sep 2001	San Clemente Island, CA	15	LACM 2001-59.1
Pisaster giganteus	2 Sep 2007	San Clemente Island, CA	14	LACM 2007-126.1
Pisaster giganteus	29 Oct 2010	Santa Rosa Island, CA	17–21	LACM 2010-81.2
Pycnopodia helianthoides	30 Jun 1942	Coos Co, OR	Inter.	LACM 1942-25.16
Pycnopodia helianthoides	30 Jun 1942	Coos Co, OR	Inter.	LACM 1942-25.16
Pycnopodia helianthoides	13 Dec 1948	Bodega Head, Sonoma Co, CA	Inter.	LACM 1948-45.22
Pycnopodia helianthoides	7 Aug 1971	Ft. Bragg, Mendocino Co, CA	55	LACM 1971-133.4
Pycnopodia helianthoides	23 Oct 1976	Bear Harbor Ranch, Mendocino Co, CA	Inter.	LACM 1976-9.22
Pycnopodia helianthoides	24–26 Oct 1980	Morro Bay, CA	Inter.	LACM 1980-174.2
Pycnopodia helianthoides	6 Sep 1987	Wickaninish Bay, Vancouver Island, British Columbia	45	LACM 87-114.10
Pycnopodia helianthoides	6 Sep 1987	Wickaninish Bay, Vancouver Island, British Columbia	45	LACM 87-114.10
Pycnopodia helianthoides	15 Oct 1991	San Miguel Island, CA	16	LACM 91-135.2
Pycnopodia helianthoides	15 Oct 1991	San Miguel Island, CA	16	LACM 91-135.2
Pycnopodia helianthoides	22 Jun 1997	Diablo Canyon, San Luis Obispo Co, CA	Inter.	LACM 97-42.7
Pycnopodia helianthoides	2 Jul 2001	Astoria Canyon, Clatsop Co, OR	154	LACM 2001-61.1
Pycnopodia helianthoides	8 Jul 2001	Heceta Bank, Lane Co, OR	110	LACM 2001-60.1
Pycnopodia helianthoides	17 Jun 2006	Santa Barbara Island, CA	17	LACM 2006-66.1
Pycnopodia helianthoides	2 May 2008	San Miguel Island, CA	21	LACM 2008-52.1
Pycnopodia helianthoides	24 Oct 2010	Santa Rosa Island, CA	17–21	LACM 2010-81.1
Pisaster ochraceus	29 Jan 1939	White Cove, Santa Catalina Island, CA	73-146	LACM 1939-5.10
Pisaster ochraceus	1 Jun 1941	Tomales Point, CA	Inter.	LACM 1941-373.1
Pisaster ochraceus	1 Jun 1941	Tomales Point, CA	Inter.	LACM 1941-373.1
Pisaster ochraceus	25 Jul 1942	Coast Guard Station, Coos Bay, OR	Inter.	LACM 1942-44.1
Pisaster ochraceus	25 Jul 1942	Coast Guard Station, Coos Bay, OR	Inter.	LACM 1942-44.1
Pisaster ochraceus	25 Jul 1942	Coast Guard Station, Coos Bay, OR	Inter.	LACM 1942-44.1
Pisaster ochraceus	25 Jul 1942	Coast Guard Station, Coos Bay, OR	Inter.	LACM 1942-44.1
Pisaster ochraceus	25 Jul 1942	Coast Guard Station, Coos Bay, OR	Inter.	LACM 1942-44.1
Pisaster ochraceus	25 Jul 1942	Coast Guard Station, Coos Bay, OR	Inter.	LACM 1942-44.1
Pisaster ochraceus	25 Jul 1942	Coast Guard Station, Coos Bay, OR	Inter.	LACM 1942-44.1
Pisaster ochraceus	25 Oct 1976	Half Moon Bay, CA	Inter.	LACM 1976-10.26
Pisaster ochraceus	22 Nov 1988	SE of Point Conception, CA	Inter.	LACM 88-131.45
Pisaster ochraceus	1 Jul 1991	Curry Co, OR	Inter.	LACM 91.37.1
Pisaster ochraceus	1 Jul 1991	Curry Co, OR	Inter.	LACM 91.37.1
Pisaster ochraceus	26 Jun 1994	Sonoma Co, CA	Inter.	LACM 94-73.1
Pisaster ochraceus	22 Jun 1997	Diablo Canyon, San Luis Obispo Co, CA	Inter.	LACM 97-42.8
Pisaster ochraceus	8 Sep 2006	San Miguel Island, CA	14–21	LACM 2006-75.1
Pisaster ochraceus	2 Jul 1991	Cape Ferrelo, Curry Co, OR	Inter.	LACM-91-38.1
Pisaster ochraceus	2 Jul 1991	Cape Ferrelo, Curry Co, OR	Inter.	LACM-91-38.1
Pisaster ochraceus	26 Jun 1994	Sonoma Co, CA	Inter.	LACM 94-73.1
Pisaster ochraceus	22 Jun 1997	Diablo Canyon, San Luis Obispo Co, CA	Inter.	LACM 97-41.4

Co, County; Inter., intertidal; n/a, not available; NE, northeast; S, south; SE, southeast.